Astron. Astrophys. 268, 765–774 (1993)

ASTRONOMY AND ASTROPHYSICS

Investigation of microturbulent magnetic fields in the solar photosphere by their Hanle effect in the Sr I 4607 Å line

M. Faurobert-Scholl

Observatoire de la Côte d'Azur, Laboratoire G.D. Cassini, CNRS URA 1362, B.P. 229, F-06304 Nice Cedex 4, France

Received April 16, accepted July 15, 1992

Abstract. Stenflo (1982) suggested that unresolved turbulent magnetic fields in the solar photosphere could be detected by their depolarizing Hanle effect and advanced a lower limit of 10 G from an approximate analysis of a few photospheric lines.

This paper addresses the same question with a detailed analysis of the center-to-limb variations of the Sr I 4607 Å line, recorded by Stenflo et al. (1980). The effect of multiple scattering, depolarizing collisions and partial frequency redistribution are fully taken into account. In spite of large uncertainties in the value of the collisional cross-section of neutral strontium with neutral hydrogen, we find that the observed polarization rates are hard to explain without depolarizing effects, which following Stenflo (1982) we ascribe to a weak turbulent magnetic field producing depolarization by Hanle effect.

As the spatial scale of a weak turbulent magnetic field is likely to be smaller than 300 km, which is a typical mean free path for a Sr I 4607 Å line photon at the top of the photosphere, the effect of the turbulent magnetic field is treated in the microturbulent limit. In the transfer equation for the Stokes parameters, the Hanle phase matrix is thus replaced by its average over the magnetic field distribution. We show that the center-to-limb observations of the Sr I 4607 Å line polarization indicate the presence in the photosphere of a depth-dependent turbulent magnetic field. Its intensity decreases from values in the range 30 G to 60 G at the altitude $z = 150$ km above $\tau_{5000} = 1$, to values in the range 10 G to 30 G at the altitude $z = 250$ km. It then remains roughly constant at higher altitudes.

Key words: lines: formation – polarization – Hanle effect – photospheric magnetic fields

1. Introduction

This paper deals with the problem of the diagnostic of weak turbulent magnetic field in the solar photospere. It seems now well established that most of the magnetic flux through the photosphere occurs in strong, kilogauss form, in very concentrated magnetic elements, the so-called fluxtubes, which cover less than one percent of the solar surface (Stenflo 1989). The remaining part of the atmosphere is certainly not completely field free. Stenflo (1982) suggested that a large amount of magnetic flux could be hidden from view in magnetograms if opposite polarity fluxes are mixed over small scales which are below the present spatial resolution of observations.

In the presence of a mixed polarity magnetic field the circular polarization due to Zeeman effect averages out to zero, but other effects, such as the Zeeman broadening of line profiles, the transverse Zeeman effect and the Hanle depolarization can still be detected. Up to now the "turbulent" field has not yet been positively identified but the analysis of these effects have provided some observational constraints on its properties. The linear polarization, due to Zeeman transverse effect, gives information on the angular distribution of the magnetic field. The analysis of the available observations suggests that the field distribution is almost isotropic (Stenflo 1984, 1987). The line broadening technique has given an upper limit of 100 G for its intensity (Stenflo & Lindegren 1977).

It was first pointed out by Stenflo that the presence of such a weak mixed polarity magnetic field in the solar photosphere should produce a detectable Hanle effect on the linear resonance polarization which is observed in some photospheric absorption lines. Linear polarization of photospheric absorption lines formed outside active regions has been systematically investigated by Stenflo et al. (1983a, b). The origin of this non-magnetic polarization is the coherent scattering of the anisotropic photospheric radiation field by the atoms. The absorption of an anisotropic radiation field leads to atomic polarization of the excited level, i.e. non-uniform population of Zeeman sub-levels and phase relationship between these sub-levels. If the atomic polarization is not destroyed, for example by elastic depolarizing collisions, before radiative decay of the atom, then the re-emitted radiation field is linearly polarized (Mitchell & Zemansky 1934; Stenflo 1976). This is the so-called resonance polarization. In the presence of a weak magnetic field, such that the energy shift between the Zeeman sub-levels is of the order of their width, coherences are partially destroyed. The re-emitted radiation field is still linearly polarized but the polarization plane is rotated and the polarization rate decreases. This is known as the Hanle effect (see Lamb 1970; Stenflo 1978; Bommier & Sahal-Bréchot 1978). The sensitivity domain to this effect for spectral lines in the visible spectrum covers typically magnetic intensities between a few Gauss and a hundred Gauss. In a mixed polarity magnetic field with isotropic distribution of the field vectors, there is no preferred direction of rotation but the Hanle effect depolarization is never cancelled out.

The linear polarization profiles observed in photospheric lines outside active regions should thus provide a well suited observational diagnostic for weak mixed polarity magnetic field in the

Send offprint requests to: M. Faurobert-Scholl

photosphere. A first approximate analysis of these profiles has been carried out by Stenflo (1982). In order to avoid the solving of the full polarized line transfer problem he assumed that polarization is due only to the last scattering of line photons in the photosphere and he used approximate expressions to represent the anisotropy of the line radiation field. The rate of depolarizing collisions was also given approximate values. This "qualitative" treatment of the problem, achieved for a number of polarized lines, provided crude estimates of the magnetic intensity and led to a lower limit of 10 G for the intensity of the turbulent magnetic field.

A more precise determination of the turbulent magnetic field requires an accurate treatment of the polarized line formation. The reason is that resonance polarization is very sensitive to multiple scattering and to the details of non-LTE mechanisms, such as depolarizing collisions, which play a role in the formation of the line. In order to clearly identify the presence of a turbulent magnetic field and to obtain constraints on its intensity it is of crucial importance to calculate as exactly as possible the amount of depolarization due to collisions and multiple scattering as well as that due to a weak mixed polarity magnetic field.

The aim of this paper is to carry out detailed calculations of Hanle depolarization due to a weak turbulent magnetic field on a "well chosen" line which could lead to a clear diagnostic of turbulent magnetic field in the photosphere. The line which will be studied here is the resonance line of neutral strontium at 4607 Å. The center to limb variations of its linear polarization have been recorded by Stenflo et al. (1980). This line which is due to a dipole type transition shows a relatively high core polarization and is not affected by blends. Its maximum of sensitivity to the Hanle effect is obtained for magnetic intensities of about 20 G (see Sect. 3). The numerical tools which are necessary for a self-consistent description of the effects on resonance polarization of both multiple scattering and weak deterministic magnetic fields have been developed in Faurobert-Scholl (1991). These tools have then been generalized to include the effect of depolarizing collisions and applied to the interpretation of the linear polarization of the solar Ca I 4227 Å absorption line in Faurobert-Scholl (1992). We now want to address the problem of Hanle effect due to turbulent magnetic fields. We thus have to face a fundamental problem: how shall we write the transfer equation in that situation?

As in the case of lines formed in the presence of turbulent motions, the polarized transfer equation in the presence of turbulent magnetic fields in no more a deterministic equation but a stochastic equation because the phase matrix which describes the correlations in direction and polarization between the absorbed and re-emitted photons, contains stochastic coefficients. The polarization profiles will thus also be stochastic. The observable quantity in this case is the average of the profiles over a large number of realizations of the turbulent magnetic field. In the most general case the only "exact" numerical solution of the transfer problem would then be obtained by means of Monte-Carlo techniques and this would be very time consuming. However, there are two limiting cases where the observable profiles may be obtained through the solution of non-stochastic equations. These limits are the so-called "microturbulent" and "macroturbulent" cases. Microturbulence refers to situations where the scale of the turbulent field is much smaller than the typical mean free path of line photons. In this limit the mean profiles satisfy the transfer equation with the averaged coefficients. This is a well known situation for turbulent motions (see Mihalas 1978, p. 463) and is easily extended to the case of turbulent magnetic fields. On the contrary, macroturbulence refers to situations where the scale of the turbulent field is much larger than the mean free path of line photons. In that case for each realization the magnetic field is uniform. The observable profiles are an average of the emergent profiles over all the possible values for this uniform magnetic field.

We shall see that for the Sr I 4607 Å line, the typical mean free path of line photons at the top of the photosphere is about 300 km. The microturbulent limit is thus valid if the scale of the turbulent magnetic field is smaller than 300 km. There is up to now no observational lower limit for the scale of the turbulence and the theoretical lower limit corresponds to the ohmic diffusion scale, which is of order 1 km (Stenflo 1989). In the following we shall only consider microturbulent magnetic fields. This is obviously the most simple case which has to be first investigated.

In this paper we first calculate the linear polarization in the Sr I λ4607 Å solar line in the absence of magnetic field. Elastic collisions are modelled according to the van der Waals approximation. A difficulty arises here because the van der Waals coefficient for this line is not known. In paper II we obtained an empirical determination of the van der Waals coefficient for the Ca I 4227 Å resonance line, denoted by γ_w(Ca) in the following. According to the approximate expression given by Allen (1964) for the van der Waals coefficient, the relevant value for the Sr I 4607 Å resonance line, which we denote by γ_w(Sr), should be very close. The reason is that the atomic configuration of Sr I is very similar to the one of Ca I. The center-to-limb variations of the linear polarization at line center are calculated for a set of values of the van der Waals coefficient ranging from γ_w(Ca) up to $4\gamma_w$(Ca) and compared to the observations of Stenflo et al. (1980). Let us stress that in order to compare computed rates with those which have been recorded by Stenflo et al. it is necessary to model quite accurately the macroturbulent and instrumental line broadening which decreases the polarization rates at line center. This is well constrained by the observations, because of observed Sr I line width is dominated by macroturbulent and instrumental broadening. On the other hand, microturbulent motions are not so well constrained. We shall see that a VAL3C-like microturbulent velocity leads to smeared intensity profiles which are very close to those obtained if we adopt, following Holweger et al. (1991), a depth-independent microturbulent velocity of 1 km s^{-1}. On the other hand, the smearing effect due to macroturbulence and finite spectral resolution leads to quite different amounts of line core resonance polarization at the limb in both cases.

Results obtained with the VAL3C microturbulent velocity and with a depth-independent microturbulent velocity of 1 km s^{-1} are shown. In both cases, it clearly appears that the center-to-limb variations of the observed polarization rates cannot be explained without considering Hanle effect depolarization.

We then calculate the effect of microturbulent magnetic fields, with depth-independent statistical properties, on the linear polarization of the Sr I 4607 Å line. We show that the ratio q/q^0, where q and q^0 are the values of the Stokes parameter Q at line center with and without magnetic field, is independent of the adopted microturbulent velocity. On the other hand this ratio, which measures the amount of depolarization due to the turbulent field, is significantly affected by multiple scattering of line photons in the photosphere. We show that the depolarizing effect of the magnetic field is enhanced by multiple scattering. An analytical evaluation of the effect of multiple scattering, obtained from methods which are close to escape probability methods, is proposed. It is in good agreement with the numerical results. Finally we show that the center-to-limb observations of Stenflo et al. can be interpreted in terms of the existence in the photosphere of a depth-dependent turbulent magnetic field. If we adopt typical

values for the van der Waals coefficient and a depth-independent microturbulent velocity of 1 km s^{-1}, the derived effective magnetic intensity (in a sense which will be defined later) decreases between a value of the order of 30 G to 60 G, at the altitude $z = 150$ km above $\tau_{5000} = 1$, to a value between 10 G and 30 G at $z = 250$ km, it then remains roughly constant at higher altitudes. If we adopt the VAL3C-microturbulent velocity, the depth-dependence is similar but we derive a smaller magnetic intensity in the upper photosphere.

2. Non-magnetic polarization of the Sr I 4607 Å line

The method used to calculate the non-LTE polarized line formation is the same as in Paper II. As in the case of calcium, the dominant specie of strontium in the solar photosphere is the singly ionized form Sr II and non-LTE effects are important both for the ionization equilibrium and for the formation of the absorption line. As in Paper II we use the VAL3C (Vernazza et al. 1981) semi-empirical model of the solar atmosphere both with its original depth-dependent microturbulent velocity and with a microturbulent velocity of 1 km s^{-1}. This second version of the atmospheric model will be denoted by MIC1 in the following. The two models differ mainly in the upper photosphere, where the VAL3C microturbulence decreases to values of the order of 0.5 km s^{-1}.

2.1. *Polarized line formation model*

The Sr I 4607 Å resonance line is very similar to the Ca I 4227 Å resonance line which was studied in Paper II. They are both normal triplets, due to transitions of the type $^1S_0 \rightarrow {}^1P_1$. The electronic configuration of neutral strontium belongs to the same family as that of neutral calcium, they both have two outer electrons, but strontium has one more electronic shell than calcium. As in the case of the resonance line of Ca I, a very simple atomic model of strontium can be used. Only the $^1S_0$ ground level, the excited $^1P_1$ level and the fundamental ^2S level of ionized Sr II are considered (cf. Table 1). As far as the resonance line is concerned, the coupling with the other levels of neutral strontium does not play an important role.

Details about the computation of the transition rates which appear in the equations of statistical equilibrium of the atomic levels are given in Appendix A. As in Paper II we assume that the populations of the levels do not depend on the line polarization.

Table 1. Model strontium atom.
1: Treated explicitly; 2: $T_{rad} = 5000$ K; 3: $T_{rad} = 5400$ K

	Excitation energy (eV)		Statistical weight
Sr II	5.692	^2S	$g = 2$
	2.691	$^1P_1$	$g = 3$
Sr I	0	$^1S_0$	$g = 1$

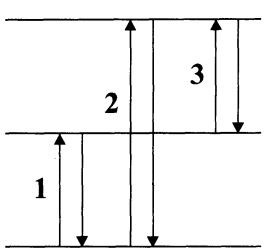

They are calculated as in ordinary non-LTE line formation problems, using an equivalent two-level iterative method and starting for the first iteration with the LTE populations. Only 2 or 3 iterations are needed to reach convergence. This first calculation provides the optical thickness in the line at each depth. The line polarization is then obtained by solving the vectorial transfer equation for the Stokes parameters. The vectorial line transfer equation is the same as in Eq. (1) of Paper II and the vectorial line source function given by Eqs. (6), (8) and (9) is written

$$\boldsymbol{S}_L(\tau, x, \boldsymbol{\Omega}) = \{\boldsymbol{sc}(\tau, x, \Omega) + (\varepsilon' \mathscr{B} + \eta B^*)\boldsymbol{U}\}/(1 + \varepsilon' + \eta), \tag{1}$$

where *sc* denotes the scattering term, $\mathscr{B}$ is the Planck function and U is the vector $(1, 0, 0)$†. We have used the same notations as in Paper II, τ is the frequency integrated optical depth, x is the frequency measured from line center in Doppler width units and $\boldsymbol{\Omega}$ is the propagation direction, defined by its colatitude θ and its azimuth φ. The source function (1) is the generalization to the vectorial case of the equivalent two-level atom formulation for a two-level atom with continuum. The additional creation term ηB^* and sink term η are due to the coupling with the continuum. Their analytical expressions, with the same notations, are given by Mihalas (1978, p. 359, 360). The sink term ε' is given by

$$\varepsilon' = \frac{\Gamma_I(1 - e^{-h\nu_0/kT_e})}{\Gamma_R}, \tag{2}$$

where Γ_I is the collisional de-excitation rate and Γ_R is the radiative de-excitation rate, these rates are given in Appendix A.

Let us examine again the scattering term. It accounts for both the effect of partial frequency redistribution and linear polarization. For a normal triplet it is written

$$\begin{aligned}\boldsymbol{sc}(\tau, x, \Omega) = \Bigg\{ & \int_{-\infty}^{+\infty} [\gamma R_{II}(x, x') + b R_{III}(x, x')]\, dx' \\ & \cdot \int \frac{d\Omega'}{4\pi} \boldsymbol{P_R}(\Omega, \Omega') \boldsymbol{I}(\tau, x', \Omega') \\ & + c \int_{-\infty}^{+\infty} R_{III}(x, x')\, dx' \\ & \cdot \int \frac{d\Omega'}{4\pi} \boldsymbol{P}_{is} \boldsymbol{I}(\tau, x', \Omega') \Bigg\} \frac{1}{\phi(x)},\end{aligned} \tag{3}$$

where $\boldsymbol{P_R}$ is the Rayleigh scattering phase matrix and $\boldsymbol{P}_{is}$ is the isotropic phase matrix. The standard notations R_{II} and R_{III} refer to the angle-averaged frequency redistribution functions corresponding respectively to coherent scattering and complete frequency redistribution in the rest frame of the atom. Obviously, only the term proportional to the Rayleigh phase matrix yields linear polarization of the re-emitted radiation field. The branching ratios are given by

$$\begin{aligned}\gamma &= \frac{\Gamma_R + \Gamma_I}{\Gamma_R + \Gamma_I + \Gamma_C}, \\ b &= \frac{\Gamma_R + \Gamma_I}{\Gamma_R + \Gamma_I + \Gamma_C} \cdot \frac{\Gamma_C - D^{(2)}}{\Gamma_R + \Gamma_I + D^{(2)}}, \\ c &= 1 - c - b.\end{aligned} \tag{4}$$

where Γ_C is the rate of elastic collisions and $D^{(2)}$ the rate of elastic collisions which destroy alignment.

As in Paper II, we assume that elastic collisions are due to collisions with neutral hydrogen atoms and we use the van der Waals approximation

$$\Gamma_C = \gamma_w(\mathrm{Sr}) n_H (T_e/5000)^{0.3}, \tag{5}$$

where γ_w(Sr) is the so-called van der Waals coefficient for neutral strontium, n_H is the density of neutral hydrogen atoms and T_e is the electronic temperature. In paper II we could determine the van der Waals coefficient, γ_w(Ca), which applies to the Ca I 4227 Å line from the interpretation of the resonance polarization observed in the line wings. We obtained a value of about $1.3\ 10^{-8}\,cm^{-3}\,rad\,s^{-1}$, which is in good agreement with previous theoretical calculations by Deridder & van Rensbergen (1976). According to the approximate expression given by Allen (1964), the van der Waals coefficient is proportional to $(\chi - W)^{-4/5}$, where $\chi - W$ is the energy required to ionize the excited level. This gives

$$\frac{\gamma_w(\mathrm{Sr})}{\gamma_w(\mathrm{Ca})} \simeq \left\{\frac{3.2}{3.0}\right\}^{4/5} \simeq 1.05. \quad (6)$$

This evaluation is also in agreement with the results of Deridder & van Rensbergen (1976).

In the case of a dipole-dipole interaction between neutral atoms, and assuming that $\Gamma_I = 0$, Berman & Lamb (1969) have shown from numerical work that the fraction of depolarizing elastic collisions is $D^{(2)}/\Gamma_C \simeq 0.379$. This result may also be used when Γ_I/Γ_R is small (Ballagh & Cooper 1977).

It will be shown in the following that partial frequency redistribution effects are not very important for the Sr I 4607 Å line. The frequency redistribution function $\gamma R_{II} + b R_{III}$ can thus be replaced by the approximate form $(\gamma + b) R_{III}$, with

$$\gamma + b = \frac{\Gamma_R + \Gamma_I}{\Gamma_R + \Gamma_I + D^{(2)}}. \quad (7)$$

2.2. *Intensity and resonance polarization profiles*

We show in Fig. 1 the behaviour of various quantities which play an important role in the line formation. The $\tau = 1$ region, where the line core is formed, is located around the altitude $z = 150$ km in the photosphere. The frequency integrated optical thickness at $\tau_{5000} = 1$ is $\tau \simeq 18$. These values are obtained with a strontium abundance relative to hydrogen set to $A_{Sr} = 8.5114\ 10^{-10}$ (Holweger 1979) and the MIC1 version of the solar model. The Doppler width varies from $2.91\ 10^9$ Hz at $\tau = 10^{-2}$ to $3.49\ 10^9$ Hz at $\tau = 18$, in the region $\tau = 1$, it is of the order of $3.00\ 10^9$ Hz which corresponds to $\Delta\lambda_D \simeq 21$ mÅ.

The observed line width varies from 118 mÅ at $\mu = 0.09$ to 94 mÅ at $\mu = 1$ (Stenflo 1992). This is much larger than the Doppler width, because the line is broadened both by macroturbulent motions in the solar atmosphere and by the finite spectral resolution of the instrument. Both phenomena lead to a smearing of the observed profiles which may be represented by the convolution of the calculated line profiles with a rectangular profile. As the observed line width is clearly dominated by the smearing effects, the characteristic width Δ associated to macroturbulence and finite spectral resolution may be determined by fitting the center-to-limb variations of the line width. This gives

$$\Delta = 57.22 - 12.22\,\mu\ (\mathrm{mÅ}). \quad (8)$$

The μ-dependence of Δ is probably due to the anisotropy of the macroturbulent motions in the solar photosphere (Solanki 1992). As the FTS observations performed by Stenflo et al. (1983) with a very good spectral resolution of less than 20 mÅ show, close to the solar limb, approximately the same Sr I line width as in the observations of 1980, it is likely that macroturbulent motions are the dominating source of broadening for observations performed close to the solar limb. Closer to disk center the line width is smaller and finite spectral resolution certainly plays a more important role.

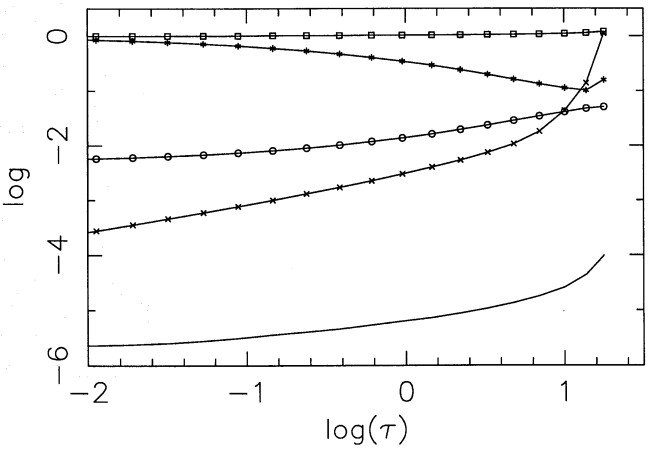

Fig. 1. Line parameters, for $\gamma_w(\mathrm{Sr}) = 1.3\ 10^{-8}$ and the MIC1 model, on a logarithmic scale as functions of the average line optical thickness τ, on a logarithmic scale. −*−: parameter γ (Eq. 4), −□−: Doppler width normalized by its value at $\tau = 10^{-2}$, −o−: Voigt parameter, −+−: parameter ε' (Eq. 2), ——: Planck function in $erg\,s^{-1}\,cm^{-2}\,sr^{-1}\,Hz^{-1}$

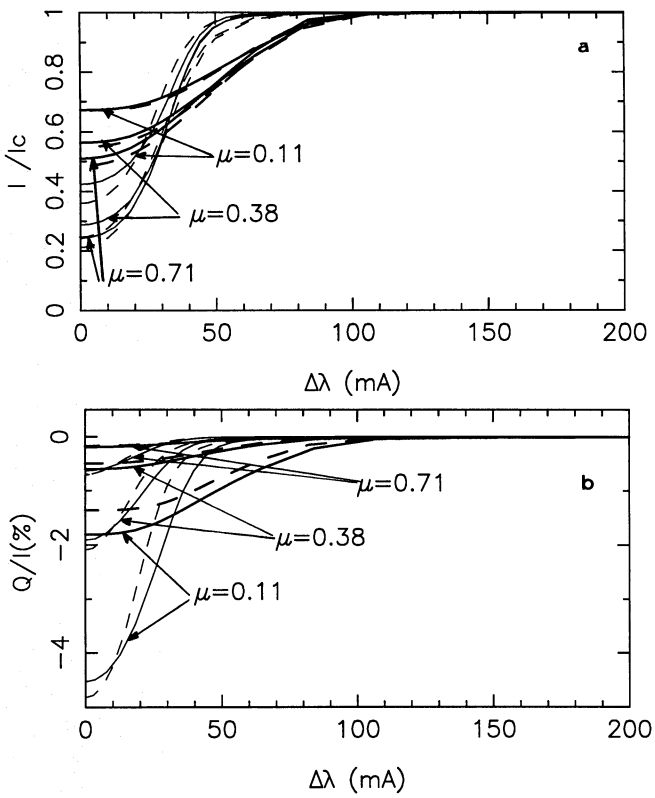

Fig. 2a and b. Intensity (in fraction of the continuum intensity) and resonance polarization rate (in %) at the surface for various values of the direction μ, as functions of the wavelength measured from line center in mÅ. Thick lines: smeared profiles, thin lines: profiles before smearing. Full lines: MIC1 model with $\gamma_w = 1.3\ 10^{-8}$, dashed lines: VAL3C model with $\gamma_w = 1.3\ 10^{-8}$

Figures 2a, b show respectively the emergent intensity and the polarization profiles in the directions $\mu = 0.11$, 0.38 and 0.71, computed with $\gamma_w(\mathrm{Sr}) = 1.3\ 10^{-8}$. The unsmeared and smeared profiles obtained with the VAL3C and M I C1 models are both

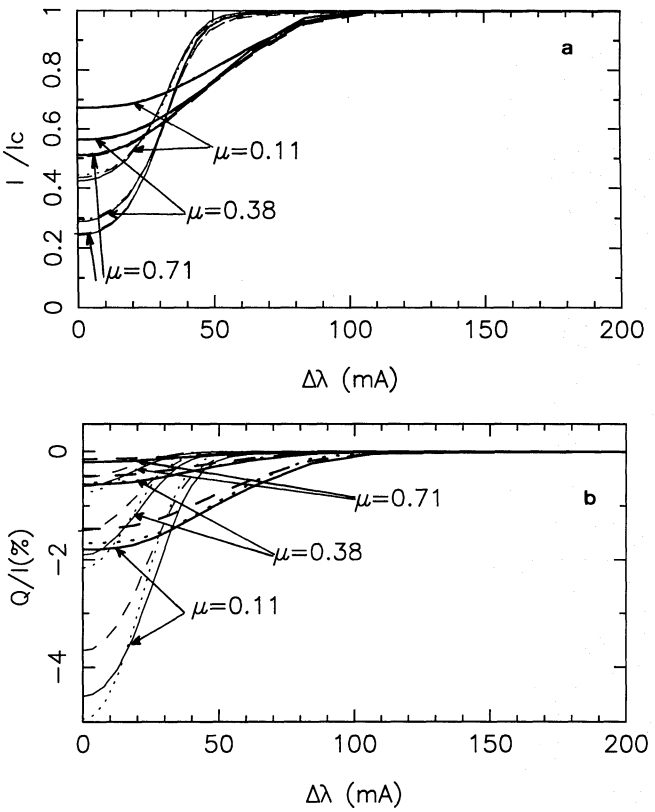

Fig. 3a and b. Same quantities as in Fig. 2a, b, but for the MIC1 model only. Thick lines: smeared profiles, thin lines: profiles obtained before smearing. Full lines: partial frequency redistribution with $\gamma_w = 1.3\ 10^{-8}$, dashed lines: partial frequency redistribution with $\gamma_w = 2.6\ 10^{-8}$, dotted lines: complete frequency redistribution with $\gamma_w = 1.3\ 10^{-8}$

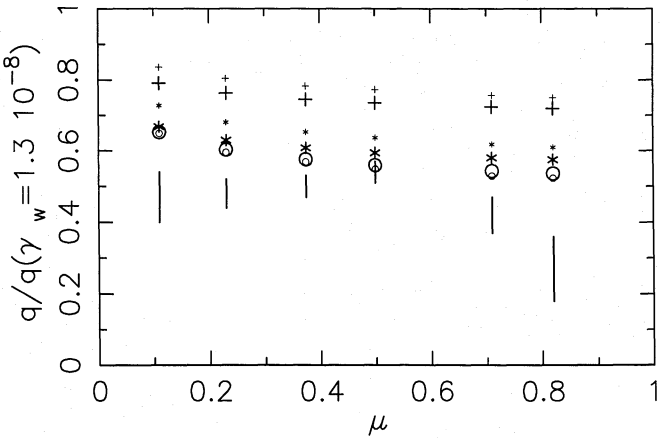

Fig. 4. Center-to-limb variations of the depolarization at line center due to elastic collisions, without smearing (thin pointers) and with smearing (thick pointers) for the M I C1 model. +: $\gamma_w = 2.6\ 10^{-8}$, *: $\gamma_w = 3.9\ 10^{-8}$, o: $\gamma_w = 5.2\ 10^{-8}$. The thick bars correspond to the observations of Stenflo et al. (1980)

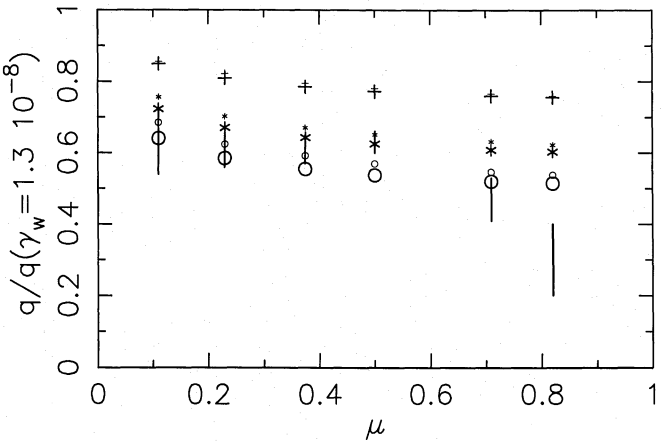

Fig. 5. Same as Fig. 4 but for the VAL3C model

shown. We see that the smeared intensity profiles are very similar in both cases, they fit the observed line width and depth within a few percent. At $\mu = 0.71$ the intensity at line center is however slightly better reproduced by the MIC1 model. The line core polarization obtained after smearing are quite different in both cases. At $\mu = 0.11$, the VAL3C model leads to $Q/I = -1.4\%$ at line center, whereas the MIC1 model gives $Q/I = -1.8\%$.

Figures 3a, b show the same quantities as in Fig. 2, for the MIC1 model only and for two values of the van der Waals coefficient, namely $\gamma_w(\mathrm{Sr}) = 1.3\ 10^{-8}$ and $\gamma_w(\mathrm{Sr}) = 2.6\ 10^{-8}$. The results obtained when complete frequency redistribution is assumed, with $\gamma_w(\mathrm{Sr}) = 1.3\ 10^{-8}$, are also shown. We see that both the intensity and polarization profiles are almost indistinguishable, after smearing, from those obtained when complete frequency redistribution is assumed. The reason is that, because of the very low value of the strontium abundance, the Sr I 4607 Å line is not a very strong absorption line and transfer of photons in the line wings, where coherence effects play a crucial role, is negligible. Figures 3 also show that the line core polarization is very sensitive to the parameter $\gamma_w(\mathrm{Sr})$ which controls the rate of depolarizing collisions, whereas the intensity profiles are much less sensitive to its value.

In Figs. 4 and 5 the center-to-limb variations of the ratio $q(\gamma_w(\mathrm{Sr}))/q(\gamma_w(\mathrm{Ca}))$, where q denotes the Stokes parameter Q at line center, are compared, for several values of $\gamma_w(\mathrm{Sr})$, with the observed values of q normalized by those which are provided by the calculations performed with $\gamma_w(\mathrm{Sr}) = \gamma_w(\mathrm{Ca})$. As, close to the limb, the polarization rates obtained with the VAL3C model are smaller than those obtained with MIC1, the observation bars corresponding to the VAL3C model (Fig. 5) lie closer to unity than those corresponding to MIC1 (Fig. 4). The behaviour of the center-to-limb variations of $q(\gamma_w(\mathrm{Sr}))/q(\gamma_w(\mathrm{Ca}))$ is also slightly different in both cases. The saturation of the depolarizing effect of collisions which appears clearly in Fig. 4 is due to the fact that when γ_w increases the line width increases and as a consequence the smearing effect of macroturbulence and finite spectral resolution becomes less efficient.

Figures 4 and 5 clearly show that the center-to-limb variations of the observed polarization in the Sr I line cannot be explained if we take into account the effect of depolarizing collisions only. In particular the relatively low values of q for $\mu \geqq 0.7$ would not be consistent with the values observed at $\mu \leqq 0.5$. We can thus conclude that the observations reveal the existence in the solar photosphere of a depolarizing mechanism different from depolarizing collisions.

In the following section we shall identify this mechanism as the Hanle depolarization due to a weak mixed polarity magnetic field and evaluate the corresponding magnetic intensity in the case of a microturbulent field.

3. Polarization in the presence of a weak microturbulent magnetic field

We recall that microturbulence refers to situations where the spatial scale of the turbulent field is small compared to the mean free path of the line photons. At the top of the photosphere, where the line polarization is formed, the mean free path of line photons is of the order of 300 km (the $\tau = 1$ region is located at the altitude $z = 150$ km). In the following we shall assume that the spatial scale of the turbulent magnetic field is smaller or of the order of 100 km. In that situation the average radiation field obeys the transfer equation where the Hanle phase matrix is replaced by its average over all the possible realizations of the magnetic field.

The average Hanle phase matrix for an isotropic distribution of magnetic fields of specified intensity has been given by Stenflo (1982) and Landi Degl'Innocenti & Landi Degl'Innocenti (1988). It may be written as

$$\langle \boldsymbol{P}_H(\boldsymbol{\Omega},\boldsymbol{\Omega}',\boldsymbol{B})\rangle_{\theta_B,\varphi_B} = W_0\,\boldsymbol{P}_{is} + \tfrac{9}{8}\,\langle M_{22}\rangle_{\theta_B,\varphi_B}\,W_2\,\boldsymbol{P}^{(2)}(\boldsymbol{\Omega},\boldsymbol{\Omega}'), \tag{9}$$

with

$$\langle M_{22}\rangle_{\theta_B,\varphi_B} = \tfrac{1}{3}\,[1 - \tfrac{2}{5}\,(S_{\rm I}^2 + S_{\rm II}^2)]. \tag{10}$$

The magnetic field enters only in the mean value of M_{22}. The notations used in (9) and (10) are the same as in paper II. We recall the W_0 and W_2 are constants which depend on the quantum numbers J and J' of the lower and upper levels of the transition, for a normal triplet $W_0 = W_2 = 1$. The matrix $\boldsymbol{P}_{is}$ is the isotropic phase matrix and $\boldsymbol{P}^{(2)}$ is given by

$$\begin{aligned}\boldsymbol{P}^{(2)}(\boldsymbol{\Omega},\boldsymbol{\Omega}') = \boldsymbol{P}_0^{(2)}(\mu,\mu') \\ + \sin\theta\,\sin\theta'\,[\boldsymbol{P}_1^{(2)}(\mu,\mu')\,\cos(\varphi'-\varphi) \\ + \boldsymbol{P}_{-1}^{(2)}(\mu,\mu')\,\sin(\varphi'-\varphi)] \\ + \boldsymbol{P}_2^{(2)}(\mu,\mu')\,\cos 2(\varphi'-\varphi) \\ + \boldsymbol{P}_{-2}^{(2)}(\mu,\mu')\,\sin 2(\varphi'-\varphi).\end{aligned} \tag{11}$$

The radiation field is axially symmetric because we are dealing with a plane-parallel atmosphere with no incident radiation and with a turbulent isotropic magnetic field. The source function depends then only on the azimuthal average of the phase matrix. When one averages (11) over the azimuthal variable φ' only the first term is remaining. This term is written

$$\boldsymbol{P}_0^{(2)}(\mu,\mu') = \tfrac{1}{2}\begin{bmatrix} \tfrac{1}{3}(1-3\mu^2)(1-3\mu'^2) & (1-3\mu^2)(1-\mu'^2) & 0 & 0 \\ (1-\mu^2)(1-3\mu'^2) & 3(1-\mu^2)(1-\mu'^2) & 0 & 0 \\ 0 & 0 & 0 & 0 \\ 0 & 0 & 0 & 0 \end{bmatrix} \tag{12}$$

The quantities $S_{\rm I}$ and $S_{\rm II}$ which appear in (10) depend on the magnetic intensity. They are given by

$$S_{\rm I} = \frac{\gamma_{\rm H}}{\sqrt{1+\gamma_{\rm H}^2}}, \qquad S_{\rm II} = \frac{2\gamma_{\rm H}}{\sqrt{1+4\gamma_{\rm H}^2}}, \tag{13}$$

with

$$\gamma_{\rm H} = 0.88\,g_J\,\frac{B}{\Gamma_{\rm R} + D^{(2)}}. \tag{14}$$

Here B denotes the magnetic intensity, measured in Gauss, g_J is the Landé factor of the upper level. The coefficients $\Gamma_{\rm R}$ and $D^{(2)}$ are given in units of $10^7\,{\rm s}^{-1}$. In this unit $\Gamma_{\rm R} = 17.8$ for the Sr I 4607 Å line. The sensitivity domain to the Hanle effect in this line, which corresponds to $\gamma_{\rm H} \simeq 1$, is for a magnetic intensity of about 20 G. Let us notice that the denominator of (14) represents the inverse life-time of the alignment of Zeeman sub-levels.

In the absence of magnetic field $\gamma_{\rm H} = 0$ hence, as shown by (10) $M_{22} = 1/3$, when $\gamma_{\rm H}$ goes to infinity $\langle M_{22}\rangle$ decreases to 1/15. When the magnetic intensity is stochastic and described by a distribution function $f(B)$, the average value of M_{22} depends on the mean value of the magnetic intensity, but also on higher moments of the magnetic intensity distribution because $S_{\rm I}$ and $S_{\rm II}$ are non-linear functions of B. For sake of simplicity, we assume in the following that the distribution function is a Dirac distribution. In this case the mean value of M_{22} is simply obtained by replacing in (10) the magnetic intensity B by a mean value, denoted by $B_{\rm t}$, which may be regarded as the effective magnetic intensity.

The transfer equation in the presence of a weak microturbulent magnetic field is almost the same as in the absence of magnetic field, except that the anisotropic part of the phase matrix is reduced by the factor r_γ, given by

$$r_\gamma = 1 - \tfrac{2}{5}\,(S_{\rm I}^2 + S_{\rm II}^2). \tag{15}$$

The numerical solution of the polarized transfer equation follows the methods developed in Paper I.

We show in Figs. 6 and 7 the center-to-limb variations of the depolarization at line center, measured by the ratio q/q^0, for a set of values of the magnetic intensity ranging from 10 G to 50 G, and for $\gamma_{\rm w}({\rm Sr}) = 1.3\ 10^{-8}$ and $2.6\ 10^{-8}$ respectively. We also show the depolarization derived from the observations of Stenflo et al. (1980). We could verify that the Hanle effect, which is measured by this ratio, does not depend on the adopted microturbulence. But, as the amount of resonance polarization, obtained in the absence of magnetic field, depends on the microturbulence (see previous section), the depolarization derived from the observations also depends on the adopted microturbulence. In Fig. 6 and 7 we show the values obtained both with VAL3C and MIC1. In both cases, the observed depolarization indicates the presence in the photosphere of a depth-dependent turbulent magnetic field whose intensity decreases when the altitude increases. If we adopt the MIC1 microturbulence and $\gamma_{\rm w}({\rm Sr}) = 1.3\ 10^{-8}$, the polarization observed in the direction $\mu = 0.82$, which is formed at the altitude of about 150 km above $\tau_{5000} = 1$, is consistent with a magnetic intensity between 40 G and 60 G. The accuracy of the determination is not very good for two reasons. One reason is the saturation of the Hanle effect when $B > 30$ G and the second one is that the polarization rate is very low (of the order of 0.03%) for this value of μ, the relative accuracy of the measurements is thus not very good (of the order of 35%). At $\mu = 0.5$, the observation corresponds to a magnetic intensity between 20 G and 30 G at the altitude of about 250 km, for smaller values of μ the observations are consistent with a magnetic field of roughly constant intensity in the range 20 G to 30 G. If we adopt the VAL3C microturbulent velocity, the depth-dependence of the magnetic intensity is similar, but we obtain lower values, in the range 10 G to 20 G, for the magnetic intensity in the upper photosphere.

Figure 7, shows the same quantities but with $\gamma_{\rm w}({\rm Sr}) = 2.6\ 10^{-8}$. We see that when the van der Waals parameter increases the depolarizing effect of a given magnetic field, which is controlled by the parameter $\gamma_{\rm H}$ defined in (14), decreases. On the other hand, the amount of resonance polarization obtained in the absence of magnetic field also decreases (see Fig. 4 and 5), so that the observed depolarization becomes closer to unity.

At $\mu = 0.82$ the magnetic intensity derived from the observation is almost the same as in the case where the van der Waals

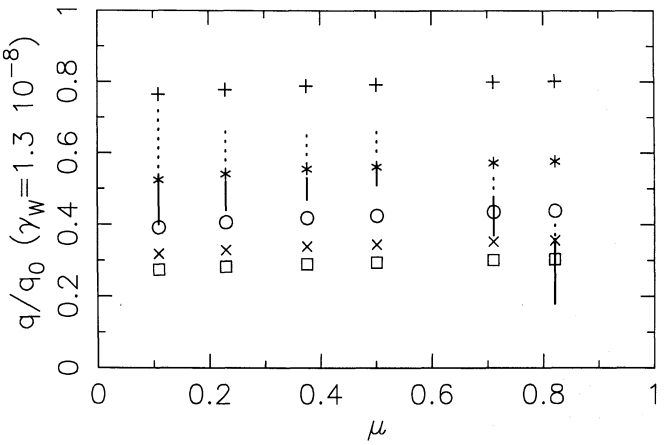

Fig. 6. Center-to-limb variations of the depolarization at line center due to the Hanle effect, in the case where $\gamma_w = 1.3\ 10^{-8}$. Only results obtained after smearing are shown. +: $B_t = 10$ G, *: $B_t = 20$ G, o: $B_t = 30$ G, ×: $B_t = 40$ G, □: $B_t = 50$ G. The depolarization derived from the observations of Stenflo et al. (1980) using the MIC1 model and the VAL3C model are represented by full and dotted bars, respectively

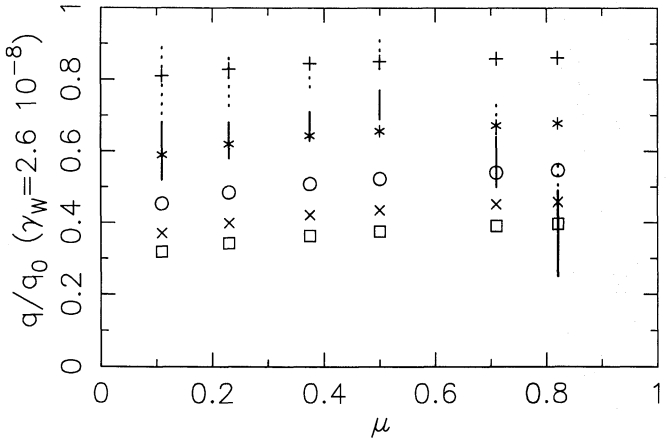

Fig. 7. Same as Fig. 5 but with $\gamma_w = 2.6\ 10^{-8}$

parameter is half smaller (see Fig. 6). This corresponds to a situation where both the Hanle effect and the resonance polarization decrease by approximately the same factor when the van der Waals parameter increases. In that case, the uncertainties on the elastic collision rate do not play an important role on the determination of the magnetic intensity.

We now show that it is possible to evaluate analytically the depolarization due to the turbulent magnetic field. We have seen in Sect. 2 that the assumption of complete frequency redistribution is a good approximation for the Sr I resonance line. As discussed in Paper I, there is a set of coupled integral equations for the two quantities $P_{00}(\tau)$ and $P_0(\tau)$ defined by

$$P_{00}(\tau) = (1-\varepsilon) \int_{-\infty}^{\infty} \phi(x')\,dx' \int_{-1}^{+1} I(\tau, x', \mu') \frac{d\mu'}{2} + \varepsilon \mathscr{B},$$

$$P_0(\tau) = (1-\varepsilon) \int_{-\infty}^{\infty} \phi(x')\,dx' \int_{-1}^{+1} \frac{d\mu'}{2} [(1-3\mu'^2)\, I(\tau, x', \mu') + 3(1-\mu'^2)\, Q(\tau, x', \mu')], \quad (16)$$

where $\varepsilon = \varepsilon'/(1+\varepsilon')$. The four other components of the vector $\boldsymbol{P}$ introduced in Eqs. (21–23) of Paper I are vanishing because the radiation field is axially symmetric. The source functions for the Stokes parameters I and Q are related to P_{00} and P_0 by

$$S_I(\tau, \mu) = P_{00}(\tau) + \tfrac{3}{8}(1-3\mu^2)\, \langle M_{22}(\tau) \rangle_{\theta_B, \varphi_B} P_0(\tau),$$

$$S_Q(\tau, \mu) = \tfrac{9}{8}(1-\mu^2)\, \langle M_{22}(\tau) \rangle_{\theta_B, \varphi_B} P_0(\tau). \quad (17)$$

In the presence of a microturbulent magnetic field Eq. (39) of Paper I is written

$$P_{00}(\tau) = (1-\varepsilon) \int_0^{\infty} K_{11}(|\tau - \tau'|)\, P_{00}(\tau')\,d\tau' + \tfrac{3}{8}(1-\varepsilon) \int_0^{\infty} K_{12}(|\tau - \tau'|)\, r_\gamma(\tau')\, P_0(\tau')\,d\tau' + \varepsilon \mathscr{B},$$

$$P_0(\tau) = \tfrac{8}{3}(1-\varepsilon) \int_0^{\infty} K_{21}(|\tau - \tau'|)\, P_{00}(\tau')\,d\tau' + (1-\varepsilon) \int_0^{\infty} K_{22}(|\tau - \tau'|)\, r_\gamma(\tau')\, P_0(\tau')\,d\tau'. \quad (18)$$

The kernels K_{11}, K_{12}, K_{21} and K_{22} are defined in Paper I. The difference with the case of zero magnetic field appears in the second integral terms where P_0 is multiplied by r_γ.

Applying the Eddington-Barbier approximation to the emergent polarization with and without magnetic field, we can relate the depolarization at line center to the ratio of the source functions S_Q at the relevant optical depth, this gives

$$\frac{q(\mu)}{q^0(\mu)} \simeq \left\{ r_\gamma(\tau) \frac{P_0(\tau)}{P_0^0(\tau)} \right\}\Big|_{\tau_0 = \mu}, \quad (19)$$

where τ_0 denotes the optical depth at line center. We recall that the superscript 0 indicates that $B_t = 0$. Let us notice that even in the presence of a depth-independent magnetic field the quantity r_γ is depth-dependent, because the rate of elastic collisions, which appears in the definition of the parameter γ_H, is depth-dependent.

From the numerical solution of the transfer equation it is clear that the intensity and P_{00} depend only very weakly on the magnetic field. So we look for a solution of (18) on the form

$$P_{00}(\tau) = P_{00}^0(\tau)$$

$$P_0(\tau) = \frac{\alpha(\tau)}{r_\gamma(\tau)} P_0^0(\tau), \quad (20)$$

where α is a function of τ to be determined. Substituting these expressions in (18) and subtracting the equation for $P_0^0(\tau)$ we obtain

$$\left(\frac{\alpha(\tau)}{r_\gamma(\tau)} - 1\right) P_0^0(\tau) = (1-\varepsilon) \int_0^{\infty} K_{22}(|\tau - \tau'|)\, (\alpha(\tau') - 1) P_0^0(\tau')\,d\tau'. \quad (21)$$

We shall now perform an approximate evaluation of the integral term by applying the same technique as in Faurobert-Scholl & Frisch (1989) where escape probability approximations were generalized to resonance polarization. The basic idea is that the quantity $(\alpha(\tau) - 1) P_0^0(\tau)$ which is identical to $r_\gamma(\tau) P_0(\tau) - P_0^0(\tau)$, varies smoothly on the optical depth interval where the line core is formed. It can thus be extracted from the integral in (21). Using the quantity $Q_e(\tau)$ introduced in Faurobert-Scholl & Frisch (1989), and which is defined by

$$\int_0^{\infty} K_{22}(|\tau - \tau'|)\,d\tau' = 0.7 - Q_e(\tau), \quad (22)$$

Table 2. Depolarization at line center in the presence of a microturbulent magnetic field of effective intensity B_t with $\gamma_w(\mathrm{Sr}) = 1.3\ 10^{-8}$. The numerical results with and without smearing are compared, for 3 values of the direction μ, with those derived from approximation (24) and from the single scattering approximation

B_t(G)	10	20	30	40	50
$q(\mu=0.11)/q^0(\mu=0.11)$ (unsmeared)	0.74	0.48	0.35	0.28	0.25
$q(\mu=0.11)/q^0(\mu=0.11)$ (smeared)	0.77	0.52	0.39	0.31	0.28
Approximation (24)	0.72	0.46	0.34	0.27	0.23
Single scattering approximation	0.80	0.57	0.44	0.36	0.31
$q(\mu=0.23)/q^0(\mu=0.23)$ (unsmeared)	0.75	0.49	0.36	0.29	0.25
$q(\mu=0.23)/q^0(\mu=0.23)$ (smeared)	0.78	0.54	0.40	0.32	0.28
Approximation (24)	0.73	0.47	0.33	0.26	0.22
Single scattering approximation	0.83	0.61	0.47	0.39	0.33
$q(\mu=0.38)/q^0(\mu=0.38)$ (unsmeared)	0.76	0.49	0.37	0.30	0.26
$q(\mu=0.38)/q^0(\mu=0.38)$ (smeared)	0.79	0.56	0.41	0.33	0.29
Approximation (24)	0.76	0.49	0.37	0.30	0.26
Single scattering approximation	0.86	0.66	0.52	0.42	0.36

we obtain

$$\alpha(\tau) \simeq \frac{r_\gamma(\tau)(0.3 + Q_e(\tau))}{1 - r_\gamma(\tau)(0.7 - Q_e(\tau))}. \quad (23)$$

The Eddington-Barbier relation (19) yields

$$\frac{q(\mu)}{q^0(\mu)} \simeq \alpha(\tau)|_{\tau_0=\mu}. \quad (24)$$

The single scattering approximation leads to

$$\frac{q(\mu)}{q^0(\mu)} \simeq r_\gamma(\tau)|_{\tau_0=\mu}, \quad (25)$$

(see Stenflo 1982).

We show in Table 2 the comparison of the numerical results with the approximations (24) and (25), for various values of μ and B_t in the case where $\gamma_w(\mathrm{Sr}) = 1.3\ 10^{-8}$. The relevant values of $Q_e(\tau)$ have been calculated as described in Faurobert-Scholl & Frisch (1989). We see that the approximation (24) reproduces quite accurately the numerical results if the smearing effect of macroturbulence and finite spectral resolution is not taken into account, whereas the single scattering approximation always underestimates the depolarization. The reason is that multiple scattering enhances the depolarization due to the Hanle effect. When smearing effects are taken into account, the depolarization decreases and the ratio q/q_0 takes values which are in the interval between those obtained with the escape probability approximation (24) and the single scattering approximation (25).

4. Conclusion

The analysis of the center-to-limb variations of the linear polarization observed by Stenflo et al. (1980) in the core of the Sr I 4607 Å absorption line indicates the presence in the photosphere of a weak depolarizing turbulent magnetic field with a depth-dependent intensity which decreases from values in the range 40 G to 60 G at the altitude of 150 km above $\tau_{5000} = 1$, to values in the range 10 G to 30 G at the altitude of 250 km. A more precise determination of the magnetic intensity at the top of the photosphere would require a better knowledge of the depolarizing collision rate and of the microturbulent velocity. At larger depths, the uncertainty is mainly due to the saturation of the Hanle effect in the Sr I line and to the decrease of the polarization rates. New observations performed with a better spectral resolution should allow to get a larger polarization signal on the solar disk and to improve the determination of the turbulent magnetic field in the low photosphere. Other photospheric absorption lines should also be studied in order to confirm these results. The analysis has been carried out under the assumption that the scale of the turbulent field is smaller than the mean free path of line photons, which is of the order of 300 km for this line at the top of the photosphere.

A rough estimate of the intensity of such a turbulent magnetic field may be obtained if we assume the equipartition of magnetic and kinetic energy at small scales. The order of magnitude of the turbulent kinetic energy at small scale is deduced from the energy contained in the solar granulation, using the assumption that the energy spectrum of granulation and microturbulence both obey the Kolmogorov law.

This point has received rather strong observational evidence recently (Roudier et al. 1991 a, b). According to this law

$$\frac{E_{mt}}{E_G} \simeq \left(\frac{\lambda_G}{\lambda_{mt}}\right)^{-5/3}, \quad (26)$$

where E_{mt} and E_G are the density of kinetic energy on the microturbulent scale, λ_{mt}, and on the granular scale, λ_G, respectively.

The equipartition between magnetic and kinetic energy at small scales gives

$$B_t^2/8\pi \simeq E_{mt} \simeq \left(\frac{\lambda_G}{\lambda_{mt}}\right)^{-5/3} E_G. \quad (27)$$

Empirical models of the solar atmosphere suggest that we can use a density of $2\ 10^{-7}$ g cm^{-3} and a velocity of the order of 1 km s^{-1} to evaluate the kinetic energy of the granules, we thus find $E_G \simeq 10^3$ erg cm^{-3}. The size of the granules is about 1000 km; if we assume that the microturbulent scale is of the order of 100 km, then (27) gives an estimate of the corresponding magnetic intensity, which should be of the order of

$$B_t \simeq 23\ \mathrm{G}. \quad (28)$$

This value is consistent with the results given by the analysis of the Hanle depolarization in the Sr I 4607 Å solar line at the top of the photosphere.

Acknowledgements. I am very grateful to Dr. Stenflo for helpful discussions and comments and for providing me with unpublished data. I also wish to thank H. Frisch, A. Pouquet and D. Galloway for stimulating discussions, and to the "Centre de Calcul Vectoriel pour la Recherche" for its support in CRAY2 computing time.

Appendix A

In this Appendix we shall explain how we compute the transition rates which appear in the statistical equilibrium equations of the atomic levels.

We use a simple atomic model of the strontium atom, which is reduced to the fundamental $5s^2\,{}^1S_0$ level, the exited $5s\,5p\,{}^1P_1$ level, and the fundamental level of Sr II. The atomic model is displayed in Table 1.

The statistical equilibrium equations are written (see Mihalas 1978, p. 359)

$$\begin{aligned} &n_1(B_{12}\bar{J}+C_{12}+C_{1k}+R_{1k})-n_2(\Gamma_R+\Gamma_I+B_{21}\bar{J})\\ &\quad -n_1(R_{1k}+C_{1k})=0,\\ &-n_1(C_{12}+B_{12}\bar{J})+n_2(\Gamma_R+\Gamma_I+B_{21}\bar{J}+R_{2k}+C_{2k})\\ &-n_2(R_{2k}+C_{2k})=0. \end{aligned} \tag{A1}$$

with

$$\bar{J}=\int_{-\infty}^{+\infty}\phi(\nu)J_\nu d\nu. \tag{A2}$$

The conservation of the total number of strontium atoms is written

$$n_1+n_2+n_k=A_{Sr}n_H^t. \tag{A3}$$

In (A 1–A 3) n_1, n_2 and n_k denote the density of strontium atoms on the fundamental level, on the excited level and on the ionized level, n_H^t is the total density of hydrogen, in neutral and ionized forms, and A_{Sr} is the abundance of strontium with respect to hydrogen. Holweger (1979) gives $A_{Sr}=8.511\ 10^{-10}$.

The Einstein coefficients for absorption and for stimulated emission, denoted respectively by B_{12} and B_{21}, are related to the spontaneous radiative de-excitation rate Γ_R by the well known relations (see Mihalas 1978, p. 79)

$$\begin{aligned} &g_1B_{12}=g_2B_{21},\\ &\Gamma_R=\frac{2h\nu^3}{c^2}B_{21}, \end{aligned} \tag{A4}$$

where g_1 and g_2 are the statistical weights of the levels. The radiative de-excitation rate Γ_R is related to the oscillator strength of the transition by

$$\Gamma_R=\frac{gf}{1.499\ 10^{-8}g_2\lambda^2}, \tag{A5}$$

where λ is given in μm and Γ_R in s^{-1} (see Allen 1964). For the Sr I 4607 Å line, $gf=1.7$, we thus have

$$\Gamma_R=1.78\ 10^8\,s^{-1}. \tag{A6}$$

The collisional excitation rate of level 1, denoted by C_{12}, is related to Γ_I by

$$C_{12}=\frac{g_2}{g_1}\exp(-h\nu/kT_e)\Gamma_I. \tag{A7}$$

The rate of collisional de-excitation Γ_I is computed from the formula given by van Regemorter (1962)

$$\Gamma_I=20.60\,\lambda^3\,n_e\,T_e^{-1/2}\,\Gamma_R P(h\nu/kT_e), \tag{A8}$$

where P is a tabulated function, and n_e and T_e denote the electronic density and temperature, respectively; the wavelength λ is given in cm.

For the collisional ionization rates from levels 1 and 2, the semi-empirical formula given by Mihalas (1978, p. 134), shows that C_{ik} ($i=1, 2$), is roughly proportional to the inverse of the ionization threshold energy, E_0^i, with a coefficient which depends on the electronic configuration of the atom. As the configuration of the strontium atom is very similar to that of the calcium atom, we write

$$\frac{C_{ik}(\mathrm{Sr\,I})}{C_{ik}(\mathrm{Ca\,I})}\simeq\frac{E_0^i(\mathrm{Ca\,I})}{E_0^i(\mathrm{Sr\,I})},\qquad i=1,\,2. \tag{A9}$$

The collisional ionization rates from levels 1 and 2 of Ca I were computed in Paper II.

The photoionization rates, from levels 1 and 2, may be written (see Auer et al. 1972)

$$R_{ik}=\frac{8\pi}{c^2}\,a_{\nu_0,i}\,\nu_{0,i}^3\,F(h\nu_{0,i}/kT_{r,i}),\qquad i=1,\,2, \tag{A10}$$

where $a_{\nu_0,i}$ is the photoionization cross-section at the ionization threshold from level i, $\nu_{0,i}$ is the corresponding frequency, and F is the function

$$F(x_0)=\int_{x_0}^{\infty}\frac{1}{x}\,\frac{dx}{e^x-1}. \tag{A11}$$

In (A 10) $T_{r,i}$ is the radiation temperature at the wavelength of the ionization threshold from level i. From the observations reported by Vernazza et al. (1976), we derive that $T_{r,i}=5000$ K and $T_{r,2}=5400$ K. The photoionization cross-sections at threshold depend on the electronic configuration of the atom, we shall assume that the values given by Auer et al. (1972) for the 4227 Å resonance line of neutral calcium can also be used for the strontium atom.

Finally, the downward rates R_{ki} are given by

$$R_{ki}=\frac{8\pi}{c^2}\,a_{\nu_0,i}\,\nu_{0,i}^3\,F(h\nu_{0,i}/kT_e),\qquad i=1,\,2. \tag{A12}$$

References

Allen C.W., 1964, Astrophysical Quantities, Oxford University Press, New York
Auer L.H., Heasley J.N., Milkey R.W., 1972, Kitt Peak Nat. Obs., Contribution No. 555
Ballagh R.J., Cooper J., 1977, ApJ 213, 479
Berman P.R., Lamb W.E., 1969, Phys. Rev. 187, 221
Bommier V., Sahal-Bréchot S., 1978, A&A 69, 57
Deridder G., van Rensbergen W., 1976, A&AS 23, 147
Faurobert-Scholl M., 1991, A&A 246, 469 (paper I)
Faurobert-Scholl M., 1992, A&A 258, 521 (paper II)
Faurobert-Scholl M., Frisch H., 1989, A&A 219, 338
Holweger H., 1979. In: Les éléments et leurs isotopes dans l'univers, 22nd colloquium of the University of Liège, publ. of the University of Liège, p. 117

Holweger H., Bard A., Kock A., Kock M., 1991, A&A 249, 545
Lamb F.K., 1970, Solar Phys. 12, 186
Landi degl'Innocenti M., Landi Degl'Innocenti E., 1989, A&A 192, 374
Mihalas D., 1978, Stellar Atmospheres, Freeman, San Francisco
Mitchell A.C., Zemanski M.W., 1934 (1961), Resonance Radiation and Excited Atoms. Cambridge University Press, Cambridge
Roudier T., Mein P., Muller R., Vigneau J., Malherbe J.M., Coutard C., Hellier R., 1991a, A&A 248, 237
Roudier T., Muller R., Mein P., Vigneau J., Malherbe J.M., Espagnet O., 1991b, A&A 248, 245
Solanki S., 1992 (private communication)
Stenflo J.O., 1976, A&A 46, 61
Stenflo J.O., 1978, A&A 66, 241
Stenflo J.O., 1982, Solar Phys. 80, 209
Stenflo J.O., 1984, Adv. Space Res. 4, 5
Stenflo J.O., 1987, Solar Phys. 114, 1
Stenflo J.O., 1989, A&A Rev. 1, 3
Stenflo J.O., 1992 (private communication)
Stenflo J.O., Lindegren L., 1977, A&A 59, 367
Stenflo J.O., Baur T.G., Elmore D.F., 1980, A&A 84, 60
Stenflo J.O., Twerenbold D., Harvey J.W., 1983a, A&AS 52, 161
Stenflo J.O., Twerenbold D., Harvey J.W., Brault J.W., 1983b, A&AS 54, 505
Van Regemorter H., 1962, ApJ 136, 906
Vernazza J.E., Avrett E.H., Loeser R., 1976, A&AS 30, 1
Vernazza J.E., Avrett E.H., Loeser R., 1981, A&AS 45, 635